ChemPubSoc Europe

DOI: 10.1002/cmdc.201900088

CHEMMEDCHEM Full Papers

Discovery, Optimization, and Biological Characterization of 2,3,6-Trisubstituted Pyridine-Containing M_4 Positive Allosteric Modulators

Jeffrey W. Schubert,*[a] Scott T. Harrison,[a] James Mulhearn,[a] Robert Gomez,[a] Robert Tynebor,[a] Kristen Jones,[a] Jaime Bunda,[a] Barbara Hanney,[a] Jenny Miu-Chen Wai,[a] Chris Cox,[a] John A. McCauley,[a] John M. Sanders,[b] Brian Magliaro,[c] Julie O'Brien,[c] Natasa Pajkovic,[d] Sarah L. Huszar Agrapides,[e] Anne Taylor,[e] Anthony Gotter,[f] Sean M. Smith,[f] Jason Uslaner,[f] Susan Browne,[e] Stefania Risso,[f] and Melissa Egbertson[a]

Herein we describe the discovery and optimization of a new series of 2,3-disubstituted and 2,3,6-trisubstituted muscarinic acetylcholine receptor 4 (M_4) positive allosteric modulators (PAMs). Iterative libraries enabled rapid exploration of one-dimensional structure–activity relationships (SAR) and identification of potency-enhancing heterocycle and *N*-alkyl pyrazole substituents. Further optimization led to identification of the potent, receptor-subtype-selective, brain-penetrant tool compound **24** (7-[3-[1-[(1-fluorocyclopentyl)methyl]pyrazol-4-yl]-6-methyl-2-pyridyl]-3-methoxycinnoline). It is efficacious in preclinical assays that are predictive of antipsychotic effects, producing dose-dependent reversal of amphetamine-induced hyperlocomotion in rats and mice, but not in M_4 knockout mice. Cholinergic-related adverse effects observed in rats treated with **24** at unbound plasma concentrations more than 3-fold higher than an efficacious dose in the hyperlocomotion assay were fewer and less severe than those observed in rats treated with the nonselective M_4 agonist xanomeline, suggesting a receptor-subtype-selective PAM has the potential for an improved safety profile.

Introduction

There is significant unmet medical need for a safe and efficacious treatment for the noncognitive symptoms of dementia, such as aggression and psychosis.[1] Clinical studies using xanomeline, an M_1/M_4 preferring muscarinic acetylcholine receptor (mAChR) subtype agonist, have demonstrated that targeting the muscarinic cholinergic system could be a viable approach for alleviating psychosis and behavioral disturbances in Alzheimer's disease (AD) and schizophrenia patients.[2,3] Preclinical studies using knockout animals and more selective molecules suggest the effects of xanomeline are likely mediated by the antidopaminergic effects of M_4 activation.[4] Unfortunately, clinical development of xanomeline was discontinued because of undesirable side effects attributed to poor receptor-subtype selectivity.[4–7] As a result of the clinical effects and adverse effect profile of xanomeline, there has been an effort to develop more selective compounds that activate M_4.[8–11] M_4 positive allosteric modulators (PAMs) bind to a site which is distinct from the orthosteric binding site of the endogenous ligand, acetylcholine. Targeting a less-conserved allosteric site with an M_4 PAM that potentiates endogenous ACh signaling can improve receptor-subtype selectivity, as demonstrated by several research groups which have identified potent and selective M_4 PAMs (Figure 1).[9,12–21]

Herein we describe lead identification efforts to develop a human- and rat-active M_4 PAM with properties suitable for evaluation in preclinical assays predictive of antipsychotic activity. We sought a compound with >100-fold receptor-subtype functional selectivity against human $M_{1-3,5}$ expressed in recombinant cell lines and pharmacokinetics that could achieve good central nervous system (CNS) exposure, and serve as an in vivo tool for evaluating M_4 PAM pharmacology.

[a] J. W. Schubert, Dr. S. T. Harrison, J. Mulhearn, R. Gomez, R. Tynebor, K. Jones, J. Bunda, B. Hanney, J. M.-C. Wai, Dr. C. Cox, Dr. J. A. McCauley, Dr. M. Egbertson
Department of Medicinal Chemistry, Merck & Co., Inc., West Point, PA (USA)
E-mail: jeffrey_schubert@merck.com

[b] Dr. J. M. Sanders
Department of Computational and Structural Chemistry, Merck & Co., Inc., West Point, PA (USA)

[c] B. Magliaro, J. O'Brien
Department of In Vitro Pharmacology, Merck & Co., Inc., West Point, PA (USA)

[d] Dr. N. Pajkovic
Department of Pharmacokinetics, Pharmacodynamics, and Drug Metabolism, Merck & Co., Inc, West Point, PA (USA)

[e] S. L. Huszar Agrapides, A. Taylor, Dr. S. Browne
Department of In Vivo Pharmacology, Merck & Co., Inc., West Point, PA (USA)

[f] Dr. A. Gotter, Dr. S. M. Smith, Dr. J. Uslaner, Dr. S. Risso
Department of Neuroscience Research, Merck & Co., Inc., West Point, PA (USA)

Supporting information and the ORCID identification number(s) for the author(s) of this article can be found under: https://doi.org/10.1002/cmdc.201900088.

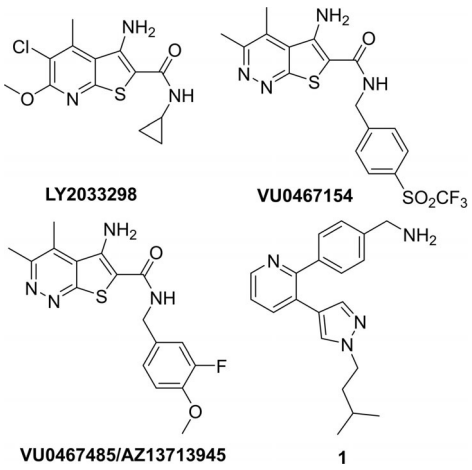

Figure 1. Structures of reported M_4 PAMs and the pyridine containing **1**, discussed herein.

Results and Discussion

M_4 is a G_i-coupled receptor, and attempts to use the native G_i signaling pathway by measuring changes in cAMP levels produced narrow signal windows that were deemed unsuitable for high-throughput screening (HTS; data not shown). Consequently, an M_4 PAM FLIPR high-throughput screen of 1.8 million compounds was conducted using CHO-K1 cells stably transfected with human M_4 receptor and Gqi5. Pyridine **1** (Figure 1) was one of few compounds with similar human and rat M_4 PAM activity (human IP = 248 nM, 106% of the maximal response to ACh (ACh Max), which is measured in the presence of 10 μM ACh; rat IP = 1.2 μM, 31% ACh Max). Compound **1** showed excellent receptor-subtype selectivity (M_{1-3} PAM all >30 μM). P-glycoprotein (P-gp) efflux ($P_{app} = 30.3 \times 10^{-6}$ cm s^{-1}; MDR1a B→A/A→B = 44.8) limited its utility as a tool compound, but the structure was an attractive lead due to its amenability to rapid analogue synthesis and the opportunity that affords to quickly explore a variety of substitutions and vectors.

Chemistry

Compounds were accessed through the generic synthetic routes outlined in Scheme 1. Suzuki–Miyaura cross-coupling between 3-bromo-2-chloropyridine **I** and *N*-alkyl pyrazole boronic acid derivatives afforded substituted pyridines **II**. Subsequent cross-coupling of **II** afforded final compounds of type **III**. To expand the scope of available cross-coupling partners from aryl boronates to aryl bromides, Stille coupling with intermediate **IV** was also pursued.

Installation of the 2-pyridyl substituent via Suzuki–Miyaura cross-coupling to give 2-aryl-3-halopyridines **VI** provided a useful intermediate for exploration of pyrazole substitution. A second cross-coupling with appropriately substituted pyrazole boronic acid derivatives afforded final compounds **VII**. Alternatively, protected pyrazole intermediate **VIII** can be deprotected and alkylated with alkyl bromides or tosylates, or with alcohols via Mitsunobu reaction.

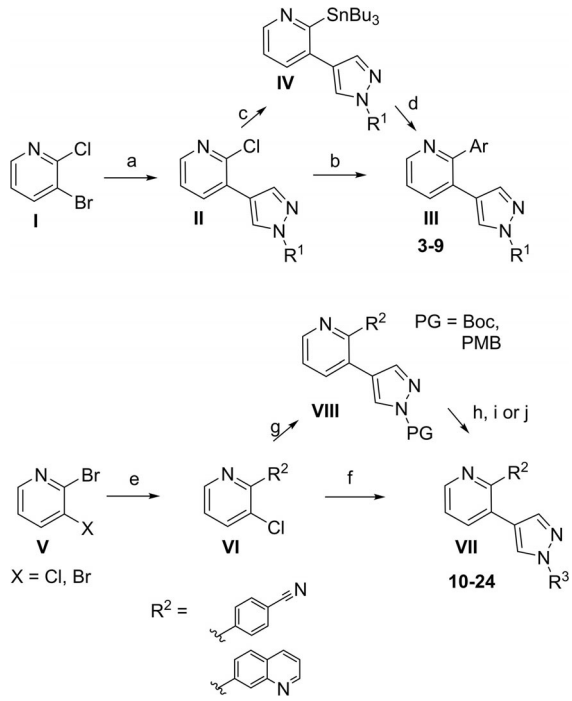

Scheme 1. Preparation of M_4 PAM analogues **III** and **VII**: a),b) ArB(pin), $Pd(dtbpf)Cl_2$, K_3PO_4, THF, 80 °C; c) $Pd(PPh_3)_4$, $(Bu_3Sn)_2$, toluene, 125 °C; d) $Pd(PtBu_2)_3$, LiCl, CuI, ArBr, dioxane, 150 °C microwave; e) ArB(pin), $Pd(PPh_3)_4$, Na_2CO_3, dioxane, 80 °C; f) ArB(pin), $Pd(dtbpf)Cl_2$, Na_2CO_3, dioxane, 80 °C; g) $Pd(OAc)_2$, Xphos, KF, dioxane, 80 °C; h) TFA, CH_2Cl_2; i) R^1OTs or R^1Br, DMF, NaH, 65 °C; j) R^1OH, DIAD, PPh_3, THF.

Alcohols provided a diverse pool of reagents that were converted into tosylates for alkylation. Further derivatized reagents, such as substituted cyclopentylmethyl tosylates, were prepared from cyclopentane carboxylic acid, as shown in Scheme 2. Fischer esterification, followed by deprotonation and trapping with an electrophile provided the methyl- or fluoro-substituted esters **XI**. Reduction and sulfonylation led to the final tosylates **XIII**.

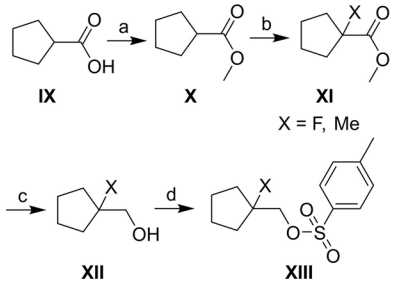

Scheme 2. Preparation of substituted cyclopentyl tosylates used for pyrazole alkylation: a) H_2SO_4, MeOH, reflux; b) X = F: LDA, NFSI, THF; X = Me: LDA, MeI, THF; c) $LiBH_4$ or $LiAlH_4$, THF d) TsCl, pyridine.

Structure–activity relationships of di- and tri-substituted pyridine M_4 PAMs

An iterative library approach as outlined in Scheme 1 enabled one-dimensional exploration of the 2-pyridyl and *N*-pyrazole

structure–activity relationships (SAR); key findings are summarized in Tables 1–3. The 4-cyanophenyl analogue **2** (Table 1) removes the basic amine and hydrogen-bond donating capacity of analogue **1**, eliminating P-gp efflux while retaining human M_4 PAM potency, improving rat M_4 PAM potency, and maintaining excellent receptor-subtype selectivity. Amide analogues derived from compound **2**, such as **3**, were generally less potent, and showed a 3- to 6-fold decrease in potency relative to the simple phenyl **4**. Naphthalene **5** and 6-substituted quinoline **6** showed large decreases in potency relative to **2**. The 7-substituted quinoline **7** exhibited slightly improved M_4 PAM potency and promising receptor-subtype selectivity (M_1 PAM IP = 1.7 μM, $M_{2,3}$ PAM > 30 μM), and led to focused exploration of heterocycles. Isoindolinone **8** and cinnoline **9** are highly receptor-subtype selective (M_{1-3} PAM all > 30 μM), exhibit similar human and rat M_4 PAM activity, and are not P-gp substrates.

Cyanophenyl **2** served as a starting point for exploration of the pyrazole substituent, summarized in Table 2. Polar ethers **10** and **11** showed a large decrease in M_4 PAM activity relative to **2**, indicating a preference for nonpolar groups in this vector. A comparison of alkyl substituents of increasing size and branching (compounds **12**–**18**) revealed that properly distanced hydrophobic bulk with nonplanar character was needed to achieve human and rat M_4 PAM activity. Linear alkyl substituents (**12**, **14**) and small aliphatic rings (**16**, **17**) demonstrated modest human M_4 PAM activity, but not rat M_4 activity, while branched alkyl (**13**, **16**), phenyl (**15**), and cyclohexyl (**18**) analogues exhibited similar human and rat M_4 PAM activity. Compound **18** is potent (human IP = 256 nM; rat IP = 229 nM) and highly receptor-subtype selective (M_{1-3} PAM all > 30 μM), but is calculated to be quite lipophilic, with Clog*D* = 4.16 at pH 7.4.

Table 1. Human and rat M_4 activity and P-gp efflux for selected M_4 PAMs.

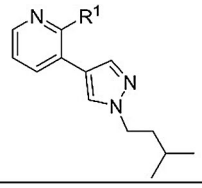

Compound	R^1	hM4 PAM IP (nM)[a]	rM4 PAM IP (nM)[a]	hP-gp (BA/AB)[b]
1	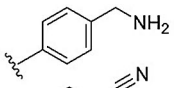	248	1233	11.1
2	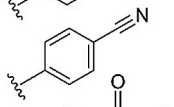	361	505	0.46
3	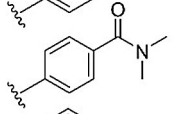	3217	6916	
4		1168	1242	0.68
5	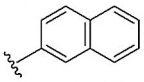	>30000	>30000	
6	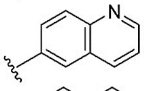	>30000	>30000	
7	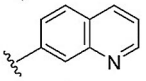	179	248	0.43
8	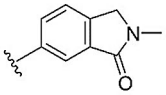	113	225	0.65
9	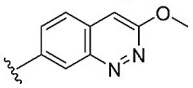	188	305	0.65

[a] Calcium mobilization assays with hM_4, rM_4, or $hM_{1,2,3}$/Gαqi5-CHO-K1 cells performed in the presence of an EC_{20} fixed concentration of acetylcholine; values represent the numerical average of at least two experiments. Inter-assay variability was 3-fold (IP, nM) unless otherwise noted. Human average ACh Max ranged from 67 to 100% for compounds **1**, **2**, **7**, and **8**, and from −18 to 57% for **3**–**6**. Rat average ACh Max ranged from −88 to 44% for **1**–**6**, and was > 84% for **7**–**9**. [b] P-gp efflux measured at 1 μM in LLC-PK1 cell line expressing rat (rat LLC-Mdr1a) or human (human LLC-MDR1) P-gp; P_{app} values in control LLC-PK1 cell line were $> 30 \times 10^6$ cm s^{-1}. Blank: not determined.

Table 2. Human and rat muscarinic activity and lipophilicity measurements for cyanophenyl-substituted M_4 PAMs.

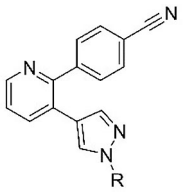

Compound	R	hM4 PAM IP (nM)[a]	rM4 PAM IP (nM)[a]	ClogD[b]
10	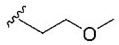	>30000	>30000	1.58
11	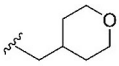	6474	9485	2.01
12		5417	>30000	2.63
13		2460	5573	2.98
14	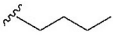	1321	>30000	3.17
15	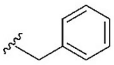	1324	2016	3.19
16		586	2260	3.33
17		372	>30000	3.04
18	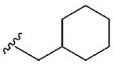	256	229	4.16

[a] Values represent the numerical average of at least two experiments. Inter-assay variability was 3-fold (IP, nM) unless otherwise noted. Human average ACh Max ranged from 35 to 45% for **10**, **12**, and **16**, and from 56 to 82% for **11**, **13**–**16**, and **18**. Rat average ACh Max ranged from −38 to 31% for **10**, **12**–**16**, and **18** and from 60 to 81% for **11**, **16** and **18**. [b] Clog*D* was calculated at pH 7.4 using ACD Percepta software (v.12).

With preliminary SAR in hand, a quinoline template was used to further probe pyrazole substitution, and efforts were focused on exploring branched alkyl substituents (Table 3). Cyclohexyl **19** was potent (human IP = 93 nM) and not a P-gp substrate but also quite lipophilic (Clog*D* = 4.73). The branched fluoroalkyl **20** was less lipophilic, but also ≈3-fold less potent. Cyclopentyl analogue **21** maintains potency and receptor-subtype selectivity, and is not a P-gp substrate. Methyl substitution of the tertiary carbon (**22**) improves M_4 PAM activity ≈3-fold, but introduces M_1 and M_2 PAM activity (IP = 1.6 μM and 170 nM, respectively). Fluoro substitution (**23**) decreases M_4 PAM potency relative to **21**, but also lowers lipophilicity (Clog*D* = 4.16) and does not impart P-gp efflux susceptibility.

Table 3. Human and rat muscarinic activity and lipophilicity measurements for quinoline-substituted M_4 PAMs.

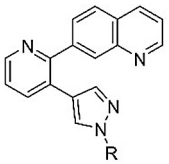

Compound	R	hM4 PAM IP (nM)[a]	rM4 PAM IP (nM)[a]	hP-gp (BA/AB)[b]	ClogD[c]
19	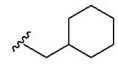	93	120	0.4	4.73
20	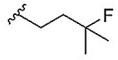	395	526		3.49
21	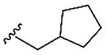	49	80	0.5	4.16
22	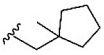	14	15		4.70
23	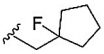	131	137	0.5	3.72

[a] Values represent the numerical average of at least two experiments. Inter-assay variability was 3-fold (IP, nM) unless otherwise noted. For all compounds, human and rat average ACh Max ranged from 88 to 100%. [b] Human P-gp efflux measured at 1 μM in human LLC-MDR1 cell line; P_{app} values were $>30\times10^{6}$ cm s^{-1}. Blank: not determined. [c] Clog*D* was calculated at pH 7.4 using ACD Percepta software (v.12).

An R-group decomposition and visualization of M_4 PAM SAR is summarized in Figure 2. Similar analyses have been previously reported,[22,23] and using these visualizations can aid in correlating structure with multiple dimensions of biological data. In Figure 2a, compounds have M_4 PAM potency ranging from 10 to 100 nM. Compounds **7**, **8**, and **9** are labeled for reference, and subsequent compounds are named following an R^3-R^2-R^1 pattern. Trends can be identified by comparing compounds within a color (R^3 = H or Me), row (R^2 = **A**, **B**, or **C**), or column (R^1 = **a**, **b**, **c**, or **d**). Using this analysis, M_4 activity is similar across subseries, with R^3 = Me equipotent or slightly more active than an unsubstituted parent, and substituted cyclopentyl congeners **c** and **d** imparting modest potency improvements.

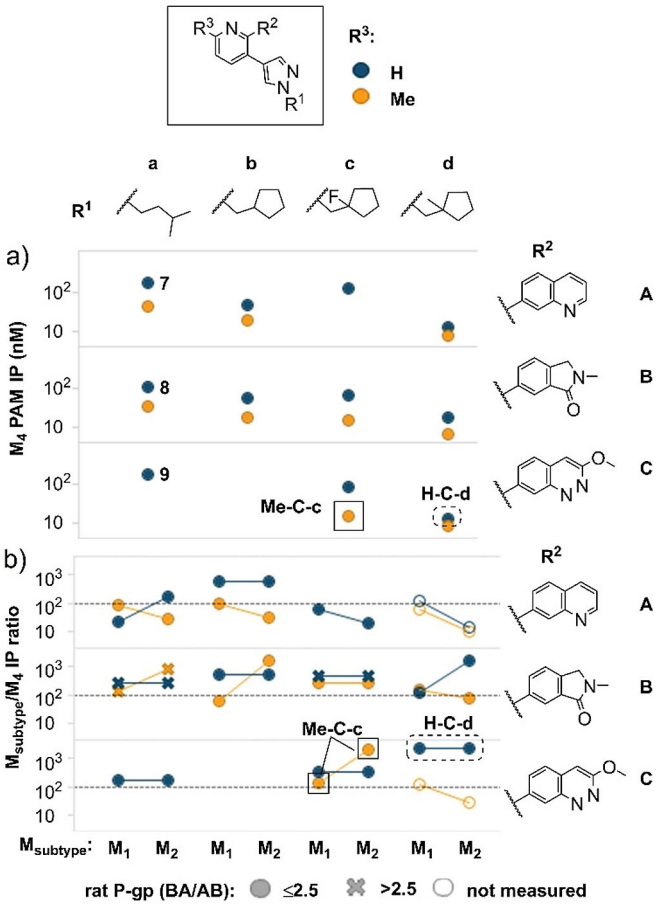

Figure 2. Graphical visualization of M_4 PAM data with biological activity and R^1 represented across the *x*-axis, R^2 across the *y*-axis, and R^3 denoted by color (H = blue, Me = orange). a) M_4 PAM potency plotted on a logarithmic scale. b) M_1 and M_2 PAM selectivity (M_1 IP/M_4 IP and M_2 IP/M_4 IP, respectively) for combinations of R^1, R^2, and R^3. Lines connect identical compounds, and markers are shaped by P-gp efflux.

Compounds were generally inactive against M_3 and M_5 (data not shown), and M_1 and M_2 receptor-subtype selectivity and P-gp efflux were used to further differentiate compounds for in vivo evaluation. Figure 2b examines receptor-subtype selectivity, with a dashed line representing 100-fold subtype selectivity and colored, solid lines connecting M_4 versus M_1 and M_4 versus M_2 selectivity for the same compound. Markers are shaped by whether or not a compound is a P-gp substrate; filled circles are not P-gp substrates, 'X's indicate P-gp substrates, and open circles do not have data (not measured).

Although not P-gp substrates, quinoline-containing compounds (**H-A-a**,**c**,**d** and **Me-A-a**,**b**,**d**) are generally less selective than isoindolinones or cinnolines, with most analogues exhibiting < 100-fold selectivity against M_1 or M_2. In two cases methyl

substitution at R^3 (compare orange and blue of **A-a** and **A-b**) lowers M_2 selectivity. By contrast, isoindolinones (**B**) and cinnolines (**C**) are generally more selective against M_1 and M_2, with most analogues exhibiting >100-fold selectivity. The effect of methyl substitution on M_2 selectivity was found to be dependent on R^1 and R^2, with increases (compare orange and blue of **B-a**, **B-b**, and **C-c**) and decreases (compare orange and blue of **B-c**, **B-d**, and **C-d**) in selectivity observed. Indeed, the interplay of selectivity imparted by combinations of R^1-R^3 highlights the utility of preparing small libraries and using a multivariate data visualization and analysis to understand trends within and between subseries.

Isoindolinone analogues were substrates for rat P-gp (**H-B-a**, **Me-B-a**, **H-C-c**), but methylation of the core (**Me-B-c**) and replacement of the pyrazole substituent (compare **H-B-c** with **H/Me-B-d**) or heterocycle (**H/Me-C-c** and **H/Me-C-d**) decreased susceptibility for P-gp. While several compounds, including **Me-C-c** and **H-C-d** (boxes, Figure 2b), meet the desired P-gp and receptor-subtype selectivity criteria, examining trends between subseries provides insight into the generality of a substituent effect. Comparing R^1=**c** versus R^1=**a**,**b**,**d** for R^2=**A** and **B** shows less variability in M_2 selectivity upon core methylation with R^1=**c**. Consequently, fluorocyclopentyl-containing PAMs (R^1=**c**) were prioritized for further characterization. Cinnoline **Me-C-c**, **24**, emerged as a compound with desired $M_{1,2,3,5}$ selectivity and M_4 PAM potency. Additionally, **24** is not a human or rat P-gp substrate. Potency, selectivity, permeability, and physicochemical properties for **24** are summarized in Table 4.

Table 4. Profile of compound **24**.

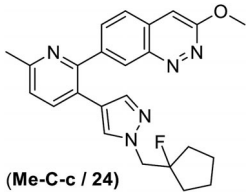

(**Me-C-c / 24**)

Parameter	Value
human M_4 PAM IP [nM]	17
rat M_4 PAM IP [nM]	29
M_1/M_4 IP ratio	134
M_2/M_4 IP ratio	>1700
M_3/M_4 IP ratio	>1700
M_5/M_4 IP ratio	>1700
P_{app} [10^6 cm s^{-1}]	32.5
Human LLC-MDR1 B→A/A→B	0.5
Rat LLC-Mdr1a B→A/A→B	0.6
Solubility (pH 2, 7, FASSIF)[a] [μM]	204, 146, 165
PSA[b] [Å^2]	68
LBE[c], LLE[d]	0.34, 4.86
HPLC log*D* (pH 7)[e]	2.89

P-gp efflux was measured at 1 μM in human LLC-MDR1 and rat LLC-Mdr1a (rat) cell lines. Average ACh Max for human and rat M_4 PAM was >95%, for human M_1 it was 60%. [a] FaSSIF: fasted-state simulated intestinal fluid. [b] Polar surface area. [c] Ligand binding efficiency: 1.4×p(hM_4 PAM IP)/HAC.[24] [d] Ligand lipophilic efficiency: p(hM_4 PAM IP)−HPLC log*D*.[24] [e] Determined by retention time using linear regression relating retention time and shake-flask log*D* values for a set of standards.

Additional pharmacological profiling shows that **24** exhibits moderate human M_4 agonism (641 nM, 45% ACh Max), but no measurable human or rat $M_{1-3,5}$ agonism (>30 μM). Testing in a rhesus M_4 PAM assay showed potency similar to rat and human (IP=13 nM). M_4 PAM **24** exhibits a favorable ancillary pharmacology profile in a screen of 119 targets (Eurofins Neuro panel), with one hit under 5 μM potency (adenosine A_1 IC_{50} 4.1 μM). NAV 1.5 activity was 7.8 μM, a >520-fold difference relative to the M_4 IP, and CAV 1.2 and MK-499 activities were >30 μM. Receptor allostery was further characterized by measuring changes in acetylcholine response (51 pM to 3 μM) at varying concentrations of **24** (100 nM to 30 μM). As shown in Figure 3, M_4 PAM **24** is a cooperative positive allosteric modulator of ACh (α=190±128) with a modest 857±613 nM affinity for the unbound receptor (KB).[25]

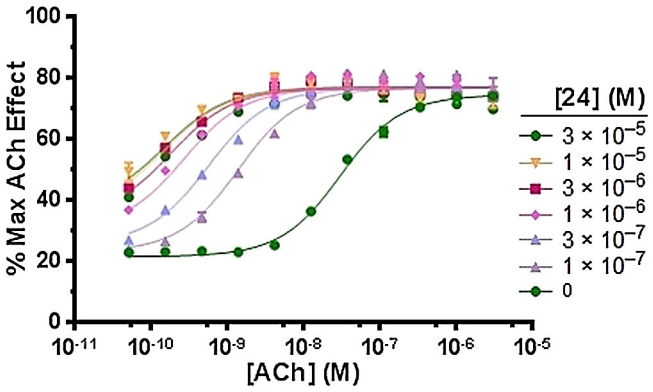

Figure 3. Acetylcholine response curves measured by Ca^{2+} flux in CHO cells expressing M_4 mAChR at varying concentrations of **24**.

With a suitable in vitro profile, pharmacokinetic studies with **24** were conducted in rat, and parameters obtained are listed in Table 5. PAM **24** is a highly permeable compound in vitro, but has poor bioavailability in rats. Subsequently, alternative routes of delivery were examined to achieve higher exposures. After intraperitoneal (i.p.) dosing in 30% Captisol, unbound plasma concentrations at 30 min and 1 h post-administration (37 and 41 nM, respectively) were ≈2- to 3-fold above the M_4

Table 5. Rat PK parameters for compound **24**.[a]

Parameter	i.v.	p.o.	i.p.
dose [mg kg^{-1}]	2	10	10
CL [mL min^{-1} kg^{-1}]	70	–	–
$t_{1/2}$ [h]	0.75	–	–
V_{dss} [L kg^{-1}]	2.4	–	–
F [%]	–	0.78	–
C_{max} [μM]	–	0.030	1.1
t_{max} [h]	–	0.38	2.0
$AUC_{0-\infty}$ [μM h]	–	0.045	8.5

[a] Intravenous and p.o. doses were administered to Wistar Hanover rats, and i.p. doses to Sprague–Dawley rats; rat PPB=4.2% unbound. Values are the mean from 2 or 3 animals; i.v. and p.o. vehicle: DMSO/PEG400/H_20 (20:60:20); i.p. vehicle: 30% Captisol.

PAM IP of **24**. Consequently, we tested pharmacodynamic response within 1–2 h of i.p. dosing, when plasma concentrations were near the M_4 PAM IP.

Pharmacology of M_4 PAM **24** was evaluated in a rat assay of amphetamine-induced hyperlocomotion, which measures animal activity in a locomotor chamber by the number of infrared beams the rat crosses over time. This assay is a surrogate preclinical assay for antipsychotic potential, as antipsychotic drugs typically abrogate stimulant-induced activity increases.[26,27] After acclimation to individual locomotor chambers for 30 min, Sprague–Dawley rats were administered vehicle or varying doses of **24** or xanomeline (5 mL kg^{-1}, i.p.); 15 min later, rats received a subcutaneous dose of amphetamine (1 mL kg^{-1}, s.c.). Motor activity recorded over the subsequent 60 min is summarized in Figure 4. Rats treated with 3, 10, and 30 mg kg^{-1} **24** exhibited a dose-dependent reversal of amphetamine-induced hyperlocomotion (Figure 4a), similar to the positive control xanomeline (10 mg kg^{-1})[27] (Figure 4b), and to other M_4 PAMs characterized by other research groups.[12,13,17,18] Unbound plasma concentrations from the highest-dose group were 25 nM at 75 min post-dose, which is ≈1.5-fold the M_4 PAM IP. Compound **24** is a permeable compound, not a substrate for rat P-gp (LLC-Mdr1a B→A/A→B = 0.6), and unbound plasma and cerebrospinal fluid (CSF) concentrations obtained from satellite animals (at 15 min) were within 1- to 3-fold of each other, suggesting sufficient CNS exposure.[28–30] Moreover, **24** dosed orally at 100 mg kg^{-1} reversed amphetamine-induced locomotion in wild-type but not in M_4 knockout mice (Figure 5). Taken together, these data suggest that **24** is an excellent tool compound for preclinical in vivo assays.

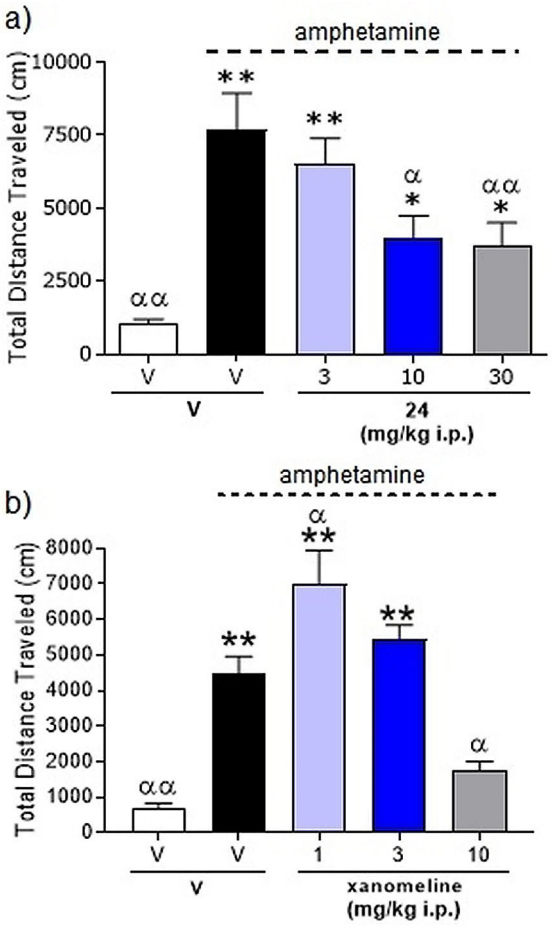

Figure 4. a) Effect of M_4 PAM **24** and b) xanomeline on amphetamine-induced locomotor activity in Sprague–Dawley rats. Data are mean ± SEM total activity measured over 60 min immediately after amphetamine administration (1 mg kg^{-1}, s.c.), $n = 7–8$ per group; $^{*}p < 0.05$, $^{**}p < 0.001$, significant differences in activity relative to control vehicle V/V treated rats; $^{\alpha}p < 0.05$, $^{\alpha\alpha}p < 0.01$ compared with activity in rats after amphetamine alone, V/amphetamine (one-way ANOVA, followed by Fisher's LSD post-hoc test).

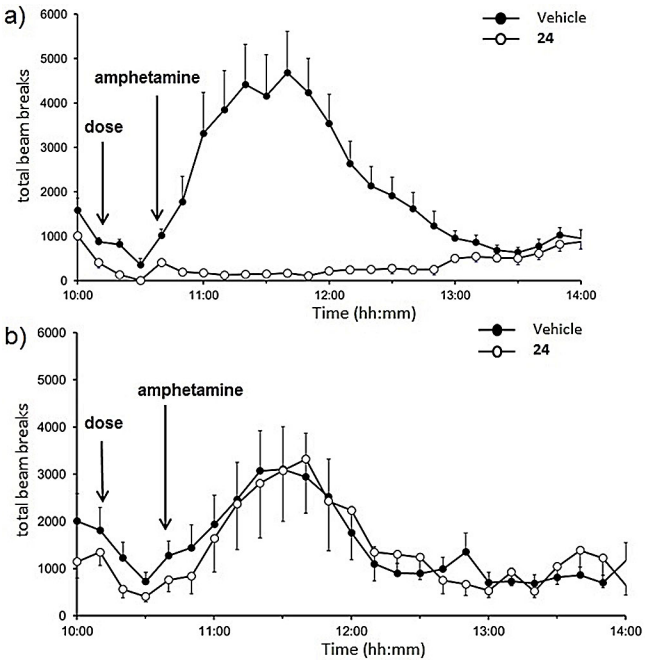

Figure 5. Data are mean ± SEM beam breaks by mice per 10-min time interval. M_4 PAM **24** reduces amphetamine-induced hyperlocomotion in wild-type mice (a), but not in M_4 knockout mice (b). Arrows indicate administration of vehicle or **24** (100 mg kg^{-1} p.o. in 30% Captisol) and amphetamine (2.5 mg kg^{-1} s.c. in saline).

The greatest perceived challenge for developing an M_4 PAM is ensuring that an adequate safety margin can be established when administrated alone and under co-administration with donepezil, the current standard of care in AD patients. Because of a lack of selectivity for M_4 over the other mAChR subtypes, xanomeline is associated with cholinergic side effects in human patients (salivation, tearing, sedation, etc.).[4] To evaluate the cholinergic side-effect potential of **24**, rats were observed following administration with the M_2 agonist oxotremorine[31] or xanomeline, which served as positive controls, or **24**, which was dosed at 10 and 100 mg kg^{-1} i.p. These doses produced unbound plasma levels that were 3.2-fold (80 nM) and 7.9-fold (198 nM) greater, respectively, than the efficacious unbound exposure observed in the rat amphetamine-induced locomotion assay. The results indicated an absence of side effects at the 10 mg kg^{-1} dose and minimal effects on sedation and pupil constriction parameters, only, at the 100 mg kg^{-1} dose (Table 6). Therefore, the improved selectivity of **24** for M_4

Table 6. Comparison of cholinergic adverse events induced in rats 30 min after treatment with behaviorally active doses of oxotremorine, xanomeline, and compound **24**.[4]

Compound:	oxotremorine	xanomeline	**24**	**24**
Dose [mg kg^{-1}]:	0.3[a]	30[b]	10[c]	100[c]
salivation	+ + (4/5)	+ + (4/5)	− (0/5)	− (0/5)
tearing	+ + (2/5)	+ (1/5)	− (0/5)	− (0/5)
piloerection	+ (4/5)	− (0/5)	− (0/5)	− (0/5)
diarrhea	+ (3/5)	+ (1/5)	− (0/5)	− (0/5)
tremors	slight/periodic (2/5)	− (0/5)	− (0/5)	− (0/5)
respiration	− (0/5)	panting/labored (2/5)	− (0/5)	− (0/5)
seizure-like activity	full body (1/5)	"absent" look (2/5)	− (0/5)	− (0/5)
sedation	+ + (3/5)	+ + (3/5)	− (0/5)	+ (2/5)
pupil constriction	+ + (5/5)	+ + (5/5)	− (0/5)	+ (1/5)

Behaviors were observed over 3 min and scored as either not present (−), mild/occasionally present (+), intermediate severity/frequently present (+ +), or severe/present constantly (+ + +) in *X*/5 rats per group. [a] 1 mL kg^{-1} s.c. in saline; [b] 2 mL kg^{-1} i.p. in saline; [c] 5 mL kg^{-1} i.p. in 30% Captisol.

versus other muscarinic receptors appears to be associated with an improved safety profile relative to the nonselective compound xanomeline.

Conclusions

In summary, pyridine HTS hit **1** was evolved into a series of potent M_4 PAMs. Comparison of M_4 PAM potency, receptor-subtype selectivity, and P-gp efflux susceptibility demonstrated interplay between pyridine and pyrazole substituents, and data visualization and multivariate analysis was used to dissect this SAR. These efforts led to the identification of **24** as a selective M_4 PAM that is efficacious in a preclinical measure of antipsychotic activity. Further optimization and pharmacological profiling of this compound series will be disclosed in due course.

Experimental Section

Compounds: Detailed synthetic procedures and characterization data can be found in the Supporting Information and a previous report.[32] All compounds were synthesized and tested at >95% purity as determined by LC–MS. All reagents and solvents were of commercial quality and used without further purification unless indicated otherwise. All reactions were carried out under an inert atmosphere of nitrogen. ^{1}H NMR spectra were obtained on a Varian Unity Inova 400 spectrometer or a Varian Unity Inova 500 spectrometer. Chemical shifts are reported in parts per million relative to TMS as internal standard. Samples provided for accurate mass measurement were taken up in methanol. The solutions were analyzed by use of electrospray ionization (ESI) or atmospheric pressure chemical ionization (APCI) on either a Bruker Daltonics 3T or 7T Fourier transform ion cyclotron resonance (FTICR) mass spectrometer. External calibration was accomplished with polypropylene glycol (425 or 750). Silica gel chromatography was carried out with an ISCO CombiFlash purification system using ISCO silica gel cartridges. Preparative reversed-phase HPLC was performed using an Agilent 1200 series chromatograph with mass-directed collection using a Waters Sunfire C_{18} column (150×19 mm I.D.) with a linear gradient over 15 min (95:5 to 5:100 H_2O containing 0.10% trifluoroacetic acid/acetonitrile.

In vitro assays: FLIPR assays were used to assess human M_{1-5}, rat M_4, and rhesus M_4 activity and were performed as previously reported.[32] M_1, M_3, and M_5 were all natively G_q coupled. Human M_4, rat M_4, rhesus M_4, and human M_2 cell lines were force coupled to Gqi5 to drive calcium mobilization. PAM activity was assessed in the presence of an EC_{20} concentration of ACh, which was determined prior to running each FLIPR assay. ACh titrations (starting with 1 μM and diluting 3-fold down for 10 points on the curve) were run on a separate plate, and the EC_{20} value was extrapolated from curves drawn within the ScreenWorks software package (Molecular Devices, LLC, San Jose, CA, USA). Typical EC_{20} concentrations for human M_4 were in the single-digit nanomolar range.

Pharmacokinetic properties: The pharmacokinetic (PK) profile of **24** was evaluated in male Wistar Hanover rats following administration of a single 2 mg kg^{-1} intravenous (i.v.) dose and a 10 mg kg^{-1} oral (p.o.) dose. In addition, PK profile following a 10 mg kg^{-1} intraperitoneal (i.p.) dose of **24** was evaluated in male Sprague–Dawley rats. Intravenous and p.o. doses were formulated as a solution in a mixture of DMSO, polyethylene glycol (PEG) 400 and water (in 20:60:20 proportions, respectively). For i.p. administration, **24** was formulated in 30% Captisol®. All animal studies were performed according to the US National Institutes of Health (NIH) Guide for the Care and Use of Laboratory Animals, and experimental protocols were reviewed by the Merck Institutional Animal Care and Use Committee.

Animals were fasted overnight with free access to drinking water and were fed 4 h after dosing. Intravenous administration to rats was done via cannulae implanted in the jugular vein, and oral formulations were administered by gavage. Blood samples were collected serially in EDTA-coated tubes up to 8 h following i.v. or p.o. dose administration, and up to 24 h following i.p. administration. Plasma was separated by centrifugation and kept frozen at −70 °C until analysis. The concentrations of test compounds in rat plasma were determined by an LC–MS/MS assay following protein precipitation and addition of an appropriate internal standard. Pharmacokinetic parameters were obtained using noncompartmental analysis using Watson LIMS®.

Plasma protein binding studies: Plasma protein binding was evaluated by equilibrium dialysis using HTDialysis plates and dialysis membranes with a 12–14 kDa MWCO (HTDialysis LLC, Groton, CT, USA). Aliquots of plasma containing test compound at 2.5 μM concentration were added to one side of the dialysis membrane and Dulbecco's phosphate-buffered saline, 1×, without calcium, mag-

nesium, phenol red, pH 7.4 (Thermo Scientific, Waltham, MA, USA) was added to the other side of the dialysis membrane. The equilibrium dialysis plate with the samples was incubated for 4 h at 37 °C, under an atmosphere of 5% CO_2. Following incubation, aliquots of the dialyzed plasma samples and buffer samples were removed from the plate, and proteins were precipitated by addition of acetonitrile containing an internal standard, followed by centrifugation. The supernatant was removed and analyzed by LC–MS/MS assay. The unbound fraction of test compounds in the plasma was determined by dividing the compound peak area over the internal standard area in the buffer by that in the dialyzed plasma samples.

Determination of bidirectional permeability in the LLC PK-1 cell line: P-glycoprotein (P-gp) transport was evaluated using similar procedures to those described elsewhere.[29] LLC-PK1 cells and LLC-PK1 cells expressing a cDNA encoding human MDR1 P-gp (human LLC-MDR1) were obtained from The Netherlands Cancer Institute (Amsterdam, The Netherlands) and used under a license agreement. LLC-PK1 cells expressing a cDNA encoding rat Mdr1a (rat LLC-Mdr1a) were made inhouse by stable transfection of LLC-PK1 cells with a rat Mdr1a cDNA. LLCPK1, human LLC-MDR1, and rat LLC-Mdr1a cell lines were cultured in 96-well trans-well culture plates (Millipore) at 37 °C in a humidified atmosphere of 5% CO_2/95% air and used in experiments after four days in culture. Solutions of test compound (final concentration 1 μM) or verapamil (1 μM, a prototypic P-gp substrate, PerkinElmer) was prepared in Hank's balanced salt solution (HBSS), 10 mM 4-(2-hydroxyethyl)-1-piperrazineethanesulfonic acid (HEPES, pH 7.4) and 1.2 μM dextran Texas red (to confirm monolayer integrity). Substrate solution (150 μL) was added to either the apical (A) or the basolateral (B) compartment of the culture plate, and buffer (150 μL; HBSS, 10 mM HEPES, pH 7.4) was added to the compartment opposite to that containing the substrate. All incubations were run in triplicate. Following 3 h incubation, 50 μL aliquots were taken from wells on both sides and analyzed by LC–MS/MS. The experiment was performed in triplicate. The reported apparent permeation (P_{app}) represents the average of the P_{app} for transport from A to B and P_{app} for transport from B to A at $t = 3$ h. The B→A/A→B ratio was calculated by dividing the P_{app} from B to A by the P_{app} from A to B.

Animals for LMA and AE studies: All animal studies were conducted in accordance with the NRC Institute of Laboratory Animal Resources Guide for the Care and Use of Laboratory Animals, and approved by the site IACUC (Merck & Co., Inc., West Point, PA, USA). Studies used adult male Sprague–Dawley rats (200–280 g, Taconic Biosciences, Germantown, NY, USA), or adult male M_4-knockout mice (20–25 g, Taconic Biosciences). Rats were housed two per cage, and mice 4–5 per cage, and animals were at controlled temperature with food and water available ad libitum under a regular 12-h light/dark cycle (18:00 lights off, 06:00 lights on). Animals were acclimated to the facility for at least one week prior to use. All studies were performed by investigators blinded to animal treatment group.

Rat and mouse locomotor activity (LMA): On the day of experiment, rats were placed individually in infrared beam-break activity boxes (Med Associates Inc., Fairfax, VT, USA) housed in a sound-attenuating chamber. Animals were allowed to habituate for 30 min before dosing i.p. with test compound **24** or xanomeline, or vehicle (30% Captisol or saline, respectively, 5 mL kg^{-1}). Rats were then returned to the activity chambers for an additional 15–30 min habituation before receiving a s.c. dose of psychostimulant amphetamine or vehicle (saline). Locomotor activity was recorded throughout, and for an additional 60 min after amphetamine administration. At the end of monitoring, blood was collected from conscious rats by tail vein draws for plasma PK analysis, and then animals were euthanized by CO_2 overdose in an induction chamber. Mice were assessed in a similar paradigm, but used Columbus Instruments infrared beam-break arrays to assess locomotor activity under home cage conditions not requiring habituation. Mouse i.p. dose volume was 10 mL kg^{-1}.

Plasma PK sample preparation: Blood was collected into 0.25 mL K_3EDTA vials and samples centrifuged at 10000 rpm for 2 min. Plasma supernatant was decanted for HPLC analysis of **24** and xanomeline.

Cholinergic adverse effects (AE) assay: On the day of testing, rats ($n = 5$ per group) were placed into individual empty rat cages and acclimated for at least 30 min before compound administration. At 30 min post-dose, animals were observed over 3 min for the appearance of AEs listed in Table 6 in a modified Irwin procedure. Data are recorded first as the number of rats per group that presented with the behavior (*X*/5 animals), and secondly as severity or duration of the behavior in the presenting animals, where − is no presentation, + is small change/occasional, ++ is medium change/frequent presentation, and +++ is maximum change/constant presentation of the behavior.

Data analysis: Total distance travelled or number of beam breaks were used to assess hyperactivity behavior. The locomotor beam box software recorded each animal's activity by beam breaks over time, and for rat data converted readouts to distance (cm) based on distance between contiguous beams crossed. Distances or beam breaks were averaged over 10 or 20 min time bins, and differences between treatment groups was analyzed using SPSS software. Comparisons of average distance or beam breaks per time bin were analyzed by repeated measure ANOVA followed by post-hoc LSD test.

Acknowledgements

*The authors thank Michael Weber and Eric Johnson for developing and running the screening assay that led to the identification of compound **1** and other novel chemical matter. We also thank Ningning Guan for initially synthesizing **1** and submitting it to the sample collection for use in screening. Janine Brouillette helped with structure determination.*

Conflict of interest

The authors declare no conflict of interest.

Keywords: muscarinic acetylcholine receptor 4 (M_4) · positive allosteric modulator (PAM) · psychosis · pyridines

[1] O. P. Tible, F. Riese, E. Savaskan, G. A. Von, *Ther. Adv. Neurol. Disord.* **2017**, *10*, 297 – 309.
[2] N. C. Bodick, W. W. Offen, A. I. Levey, N. R. Cutler, S. G. Gauthier, A. Satlin, H. E. Shannon, G. D. Tollefson, K. Rasmussen, F. P. Bymaster, D. J. Hurley, W. Z. Potter, S. M. Paul, *Arch. Neurol.* **1997**, *54*, 465 – 473.
[3] A. Shekhar, W. Z. Potter, J. Lightfoot, J. Lienemann, S. Dube, C. Mallinckrodt, F. P. Bymaster, D. L. McKinzie, C. C. Felder, *Am. J. Psychiatry* **2008**, *165*, 1033 – 1039.
[4] N. R. Mirza, D. Peters, R. G. Sparks, *CNS Drug Rev.* **2003**, *9*, 159 – 186.
[5] A. M. Bender, C. K. Jones, C. W. Lindsley, *ACS Chem. Neurosci.* **2017**, *8*, 435 – 443.

[6] J. J. Sramek, D. Pharm, D. J. Hurley, T. S. Wardle, J. H. Satterwhite, J. Hourani, F. Dies, N. R. Cutler, *J. Clin. Pharmacol.* **1995**, *35*, 800 – 806.
[7] F. P. Bymaster, D. L. McKinzie, C. C. Felder, J. Wess, *Neurochem. Res.* **2003**, *28*, 437 – 442.
[8] M. L. Woolley, H. J. Carter, J. E. Gartlon, J. M. Watson, L. A. Dawson, *Eur. J. Pharmacol.* **2009**, *603*, 147 – 149.
[9] W. Y. Chan, D. L. McKinzie, S. Bose, S. N. Mitchell, J. M. Witkin, R. C. Thompson, A. Christopoulos, S. Lazareno, N. J. M. Birdsall, F. P. Bymaster, C. C. Felder, *Proc. Natl. Acad. Sci. USA* **2008**, *105*, 10978 – 10983.
[10] T. M. Bridges, E. P. LeBois, C. R. Hopkins, M. R. Wood, C. K. Jones, P. J. Conn, C. W. Lindsley, *Drug News Perspect.* **2010**, *23*, 229 – 240.
[11] C. K. Jones, N. Byun, M. Bubser, *Neuropsychopharmacology* **2012**, *37*, 16 – 42.
[12] M. R. Wood, M. J. Noetzel, B. J. Melancon, M. S. Poslusney, K. D. Nance, M. A. Hurtado, V. B. Luscombe, R. L. Weiner, A. L. Rodriguez, A. Lamsal, S. Chang, M. Bubser, A. L. Blobaum, D. W. Engers, C. M. Niswender, C. K. Jones, N. J. Brandon, M. W. Wood, M. E. Duggan, P. J. Conn, T. M. Bridges, C. W. Lindsley, *ACS Med. Chem. Lett.* **2017**, *8*, 233 – 238.
[13] J. C. Tarr, M. R. Wood, M. J. Noetzel, J. L. Bertron, R. L. Weiner, A. L. Rodriguez, A. Lamsal, F. W. Byers, S. Chang, H. P. Cho, C. K. Jones, C. M. Niswender, M. W. Wood, N. J. Brandon, M. E. Duggan, P. J. Conn, T. M. Bridges, C. W. Lindsley, *Bioorg. Med. Chem. Lett.* **2017**, *27*, 2990 – 2995.
[14] B. J. Melancon, M. R. Wood, M. J. Noetzel, K. D. Nance, E. M. Engelberg, C. Han, A. Lamsal, S. Chang, H. P. Cho, F. W. Byers, M. Bubser, C. K. Jones, C. M. Niswender, M. W. Wood, D. W. Engers, D. Wu, N. J. Brandon, M. E. Duggan, P. J. Conn, T. M. Bridges, C. W. Lindsley, *Bioorg. Med. Chem. Lett.* **2017**, *27*, 2296 – 2301.
[15] M. F. Long, J. L. Engers, S. Chang, X. Zhan, R. L. Weiner, V. B. Luscombe, A. L. Rodriguez, H. P. Cho, C. M. Niswender, T. M. Bridges, P. J. Conn, D. W. Engers, C. W. Lindsley, *Bioorg. Med. Chem. Lett.* **2017**, *27*, 4999 – 5001.
[16] J. M. Salovich, P. N. Vinson, D. J. Sheffler, A. Lamsal, T. J. Utley, A. L. Blobaum, T. M. Bridges, U. Le, C. K. Jones, M. R. Wood, J. S. Daniels, P. J. Conn, C. M. Niswender, C. W. Lindsley, C. R. Hopkins, *Bioorg. Med. Chem. Lett.* **2012**, *22*, 5084 – 5088.
[17] M. R. Wood, M. J. Noetzel, M. S. Poslusney, B. J. Melancon, J. C. Tarr, A. Lamsal, S. Chang, V. B. Luscombe, R. L. Weiner, H. P. Cho, M. Bubser, C. K. Jones, C. M. Niswender, M. W. Wood, D. W. Engers, N. J. Brandon, M. E. Duggan, P. J. Conn, T. M. Bridges, C. W. Lindsley, *Bioorg. Med. Chem. Lett.* **2017**, *27*, 171 – 175.
[18] M. Bubser, T. M. Bridges, D. Dencker, R. W. Gould, M. Grannan, M. J. Noetzel, A. Lamsal, C. M. Niswender, J. S. Daniels, M. S. Poslusney, B. J. Melancon, J. C. Tarr, F. W. Byers, J. Wess, M. E. Duggan, J. Dunlop, M. W. Wood, N. J. Brandon, M. R. Wood, C. W. Lindsley, P. J. Conn, C. K. Jones, *ACS Chem. Neurosci.* **2014**, *5*, 920 – 942.
[19] G. Liwicki, S. Mack, P. K. Ruprah, J. Reeves (Takeda Pharmaceutical Company Limited, Japan), Int. PCT Pub. No. WO2018066718 A1, **2018**.
[20] L. Zhang, C. R. Butler, E. M. Beck, M. A. Brodney, M. F. Brown, L. A. McAllister, E. A. LaChapelle, A. M. Gilbert (Pfizer Inc., USA), Int. PCT Pub. No. WO2018002760 A1, **2018**.
[21] T. Huynh, C. Valant, I. T. Crosby, P. M. Sexton, A. Christopoulos, B. Capuano, *J. Med. Chem.* **2013**, *56*, 8196 – 8200.
[22] J. Kolpak, P. J. Connolly, V. S. Lobanov, D. K. Agrafiotis, *J. Chem. Inf. Model.* **2009**, *49*, 2221 – 2230.
[23] A. M. Wassermann, P. Haebel, N. Weskamp, J. Bajorath, *J. Chem. Inf. Model.* **2012**, *52*, 1769 – 1776.
[24] M. D. Shultz, *Bioorg. Med. Chem. Lett.* **2013**, *23*, 5980 – 5991.
[25] R. Zhang, M. Kavana, *Expert Opin. Drug Discovery* **2015**, *10*, 763 – 780.
[26] A. E. Brady, C. K. Jones, T. M. Bridges, J. P. Kennedy, A. D. Thompson, J. U. Heiman, M. L. Breininger, P. R. Gentry, H. Yin, S. B. Jadhav, J. K. Shirey, P. J. Conn, C. W. Lindsley, *J. Pharmacol. Exp. Ther.* **2008**, *327*, 941.
[27] K. J. Stanhope, N. R. Mirza, M. J. Bickerdike, J. L. Bright, N. R. Harrington, M. B. Hesselink, G. A. Kennett, S. Lightowler, M. J. Sheardown, R. Syed, R. L. Upton, G. Wadsworth, S. M. Weiss, A. Wyatt, *J. Pharmacol. Exp. Ther.* **2001**, *299*, 782.
[28] C. Tang, Y. Kuo, N. T. Pudvah, J. D. Ellis, M. S. Michener, M. Egbertson, S. L. Graham, J. J. Cook, J. H. Hochman, T. Prueksaritanont, *Biochem. Pharmacol.* **2009**, *78*, 642 – 647.
[29] K. A. Lyons, X. Shen, Z. Yao, K. Bleasby, G. Chan, M. Hafey, X. Li, S. Xu, G. M. Salituro, L. H. Cohen, W. Tang, *Xenobiotica* **2009**, *39*, 687 – 693.
[30] T. Ohe, M. Sato, S. Tanaka, N. Fujino, M. Hata, Y. Shibata, A. Kanatani, T. Fukami, M. Yamazaki, M. Chiba, Y. Ishii, *Drug Metab. Dispos.* **2003**, *31*, 1251.
[31] M. McKinney, J. H. Miller, V. A. Gibson, L. Nickelson, S. Aksoy, *Mol. Pharmacol.* **1991**, *40*, 1014.
[32] J. J. Acton, J. Bao, M. Egbertson, X. Gao, S. T. Harrison, S. L. Knowles, C. Li, M. M.-C. Lo, R. D. Mazzola, Jr., Z. Meng, M. T. Rudd, O. Selyutin, D. M. Tellers, L. Tong, J. M.-C. Wai (Merck Sharp & Dohme Corp., USA; MSD R&D China Co., Ltd.), Int. PCT Pub. No. WO2017107089 A1, **2017**.

Manuscript received: February 11, 2019
Version of record online: ■■ ■■, 0000

J. W. Schubert, S. T. Harrison, J. Mulhearn, R. Gomez, R. Tynebor, K. Jones, J. Bunda, B. Hanney, J. M.-C. Wai, C. Cox, J. A. McCauley, J. M. Sanders, B. Magliaro, J. O'Brien, N. Pajkovic, S. L. Huszar Agrapides, A. Taylor, A. Gotter, S. M. Smith, J. Uslaner, S. Browne, S. Risso, M. Egbertson*

■■ – ■■

Discovery, Optimization, and Biological Characterization of 2,3,6-Trisubstituted Pyridine-Containing M_4 Positive Allosteric Modulators

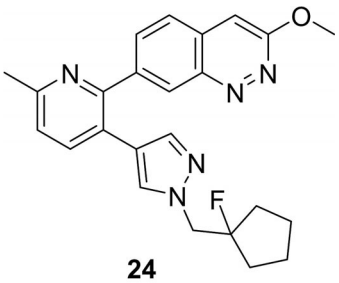

24
hM4 PAM IP:17 nM

Novel series of M_4 PAMs: Optimization of series of 2,3-di- and 2,3,6-trisubstituted pyridines led to the potent, receptor-subtype-selective, brain-penetrant positive allosteric modulator (PAM) **24** with efficacy in rodent locomotor activity assays. Comparison of cholinergic adverse effects in rats treated separately with **24** and the M_4 agonist xanomeline suggests that a receptor-subtype-selective PAM offers the potential for an improved safety profile.